Supramolecular Chemistry
Vol. 22, No. 6, June 2010, 365–379

Taylor & Francis
Taylor & Francis Group

Synthesis, binding and fluorescence studies of a new neutral H-bonding receptor for anions based on 3,5-bis(trifluoromethyl)phenylurea

Mauro Formica[a], Vieri Fusi[a]*, Luca Giorgi[a], Eleonora Macedi[a], Giovanni Piersanti[b], Maria Antonietta Varrese[b] and Giovanni Zappia[b]*

[a]*Institute of Chemical Sciences, University of Urbino, Piazza Rinascimento 6, I-61029 Urbino, Italy;* [b]*Institute of Pharmaceutical Chemistry, University of Urbino, Piazza Rinascimento 6, I-61029 Urbino, Italy*

(*Received 11 January 2010; final version received 18 February 2010*)

The synthesis and anion binding studies of the new neutral receptor 1,1′-(2,2′-(4,10-dimethyl-1,4,7,10-tetraazacyclododecane-1,7-diyl)bis(2-oxoethane-2,1-diyl))bis(3-(3,5-bis(trifluoromethyl)phenyl)urea) (**L1**) are reported. **L1** is a macrocyclic ligand containing the 3,5-trifluoromethylphenylureido-binding fragment attached as a side arm on the tetraazacyclododecane. **L1** is soluble in numerous organic solvents; the binding properties of **L1** towards several simple anions (G) were investigated by NMR, UV–vis and fluorescence techniques in DMSO and CH_3CN solutions. **L1** is able to bind F^-, Cl^- and AcO^- in both solvents; in addition, it binds Br^- in CH_3CN. Fluoride shows the highest constant values in the halide series ($F^- > Cl^- > Br^-$) and AcO^- is the most strongly bound among all the anions investigated. **L1** is able to signal the presence of the anions in solution by fluorescence change; in the case of acetate, this occurs in the visible range.

Keywords: urea; H-bonding; fluorescent sensor; macrocycles; anion recognition

Introduction

The design and synthesis of fluorogenic artificial receptors for recognition and sensing of anionic species are of current interest in the field of supramolecular chemistry (*1*). There are many factors for the rapid growth of this field including biological concerns, sensor development, environmental remediation, selective separation and extraction of chemical species and catalysis (*1b*). Several approaches to the development of anion receptors involving different interactions such as metal complexes (*2*), positively charged hosts (*3*) and neutral non-metallic H-bonding-based systems (*4*) have been reported. Urea and thio-urea have been successfully reported as neutral binding sites for anions and are widely recognised as highly useful templates upon which to build powerful recognition systems (*5*). However, *N*,*N*′-disubstituted urea compounds exhibit limited solubility in non-competitive organic solvents and often self-association through intra- and inter-molecular interactions of the NH group with the carbonyl group. Therefore, considerable effort has been devoted to the development of new urea-based receptors in order to improve their selectivity and scope (*4*).

Recently, we reported a new host (**L2**, Chart 1) able to strongly interact with acetate and simple anions such as chloride in DMSO solution (*6*). However, **L2** versatility is hampered by the scarce solubility in most of the common solvents and low optical response to the interaction with the anion. A strategy to increase the versatility of this molecular topology could be the modification of the aromatic unit linked to the ureido fragment. In the light of this, 1,1′-(2,2′-(4,10-dimethyl-1,4,7,10-tetraazacyclododecane-1,7-diyl)bis(2-oxoethane-2,1-diyl))bis(3-(3,5-bis(trifluoromethyl)phenyl)urea) (**L1**, Chart 1) has been synthesised substituting the *p*-nitrophenyl (PNP) group in **L2** with the 3,5-bis(trifluoromethyl)phenyl (TFP) unit widely employed in non-covalent organocatalysis (*7*). The choice of two trifluoromethyl moieties in place of the nitro group was based on the following: (i) it is an inert and powerful electron-withdrawing group able to increase NH polarisation of the urea; (ii) it was also proposed to rigidify the structure by polarising the adjacent H atom, which in turn facilitates a H-bonding interaction with the O atom of the ureido fragment, thus blocking unfilled H-bonding valencies; and (iii) it does not contribute to molecule self-association (*7*). In this way, the *N*-[3,5-bis(trifluoromethyl)phenyl] substituent could play the dual role to preventing aggregation/self-association by blocking H-bond donor group and providing organisation through intramolecular H-bonding.

Herein, we document the efficient synthesis of the new receptor **L1**, as well as the binding studies involving a variety of simple anions in DMSO and CH_3CN, demonstrating the ease of handling and the versatility of *N*-3,5-bis(trifluoromethyl)phenyl variations. The adaptability of **L1** in revealing anions in different solvents is

*Corresponding authors. Email: vieri.fusi@uniurb.it; giovanni.zappia@uniurb.it

ISSN 1061-0278 print/ISSN 1029-0478 online

DOI: 10.1080/10610271003731146
http://www.informaworld.com

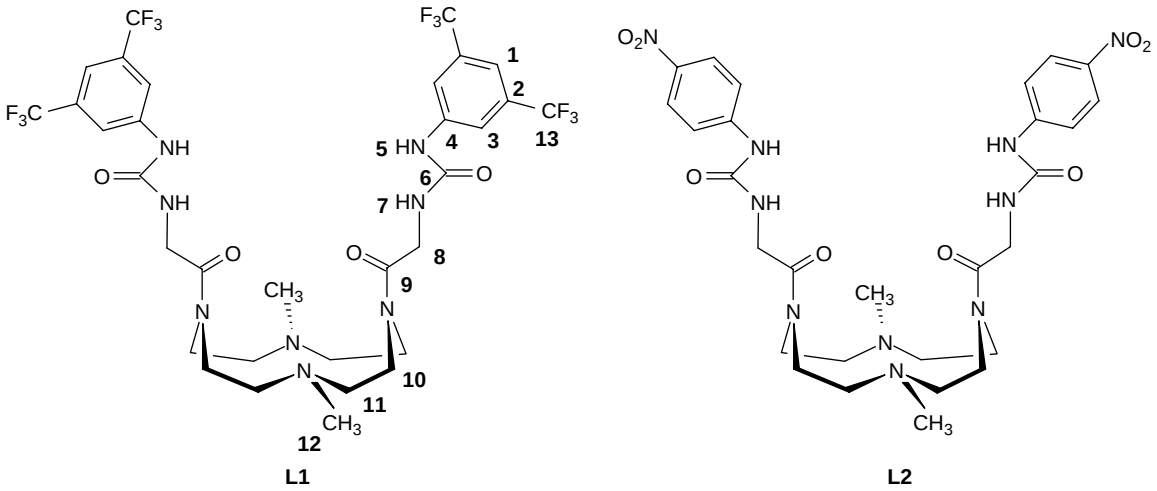

Chart 1. Ligands with labels for the NMR experiments.

highlighted by UV–vis and fluorescence in addition to classical NMR experiments.

Results and discussion

Synthesis

Scheme 1 outlines the synthesis of the new multidentate ligand **L1**. In a previous paper, we discussed the preparation of the ligand **L2**, which was based on the coupling of a protected form of glycine with 1,7-dimethyl-1,4,7,10-tetraazacyclododecane, followed by the removal of the primary amine protecting group and then by reaction with 4-nitrophenylisocyanate, with an overall yield of 32% (*6*).

The same synthetic scheme was applied for the preparation of **L1** in large scale to have enough material for the present and further studies; unforeseen, the overall yield did not exceed 20%, probably due to the reduction of the yield in the coupling process. This result prompted us to explore new and simple procedures to increase the yields for the formation of the amide bond (*8*).

During these studies, we became interested in the use of acyl fluorides as fast-acting acylating agents, introduced by Carpino et al. (*9*), which react more like activated esters than acid halides (Cl, Br and I). Other advantages of the acyl fluorides include their great stability in the presence of water, including moisture in the air, and their relative lack of conversion to the corresponding oxazolones.

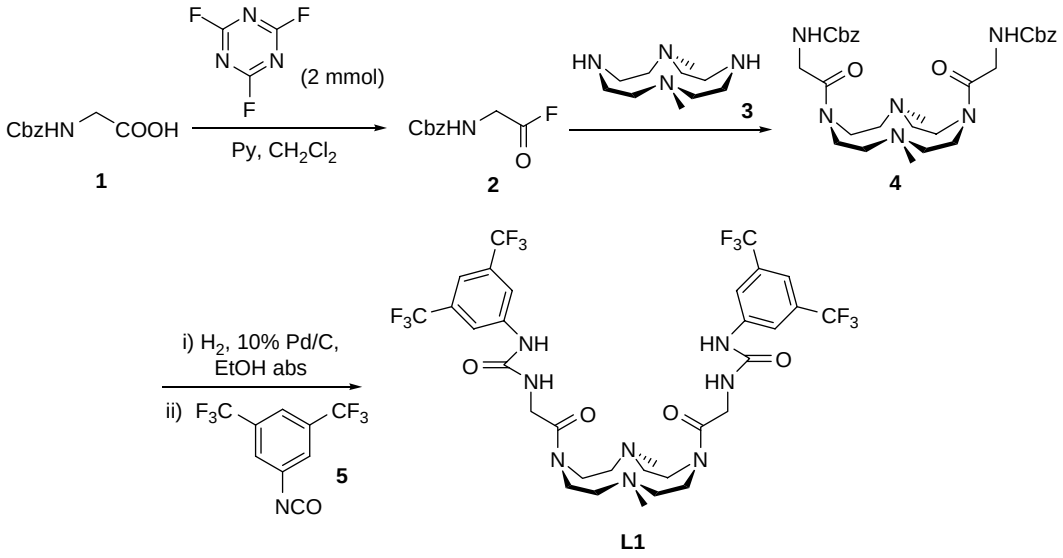

Scheme 1. Synthesis of **L1**.

Stimulated by the report by Georg et al. (*10*) on one-pot transformations of carboxylic acids to amides mediated by Deoxo-Fluor reagent, we explored the direct formation of the bis-amide by the reaction of *N*-Cbz-glycine (**1**) and 1,7-dimethyl-1,4,7,10-tetraazacyclododecane (**3**) in the presence of Deoxo-Fluor or diethylaminosulphurtrifluoride reagent. In both cases, negligible yields (10–15%) were obtained, and, in particular, with the Deoxo-Fluor reagent, the bis(methoxyethyl)amide was obtained (75% yield) as the main product by the competitive reaction of *N*-Cbz-glycine fluoride with bis(methoxyethyl) amine. We then turned our attention to the original report by Carpino for the preparation of acid fluorides using cyanuric fluoride to give *Z*-gly-F (**2**), which was coupled with 1,7-dimethyl-1,4,7,10-tetraazacyclododecane (**3**) in an aqueous biphasic system (CH_2Cl_2/H_2O–$NaHCO_3$) yielding 89%. A slightly better yield (91%) was obtained when the coupling reaction was performed in DMF, but the former conditions were selected for their simplicity.

The bis-carbamate (**4**) was then converted directly into the final ligand **L1** using a one-flash procedure.

Although, in principle, the formation of the bis-urea system in **L1** could be realised by hydrogenation of the Cbz-protecting group, isolation of the corresponding free bis-amine and final reaction with 3,5-bis(trifluoromethyl)-phenyl isocyanate (**5**), we explored a one-pot procedure to reach the same goal.

Thus, hydrogenation (H_2, 10% Pd/C) at atmospheric pressure for 4 h, followed by direct addition of isocyanate (**5**), produced compound **L1** at a satisfying yield of 61%, as an off-white solid.

Notably, **L1** is soluble in most organic solvents such as CH_3CN, $CHCl_3$ and CH_2Cl_2, but also slightly in methanol, ethanol, acetone and others, and no aggregation problems are observed.

Solution studies

The anion binding abilities of **L1** were evaluated by ^1H, ^{19}F NMR, UV–vis and fluorescence spectroscopic titrations with anions (G) such as the halide series and acetate in both DMSO and CH_3CN.

L1, unlike **L2**, is soluble in other solvents in addition to DMSO, thus widening the field of application. Table 1 reports the association constants of the adducts formed, obtained by processing the suitable spectroscopic titrations; in DMSO, only the NMR allows the evaluation of the association constants, while in CH_3CN, they can be obtained by processing the UV–vis and fluorescence titrations. The NMR is not suitable since the association constants with these anions are too high in this medium (*11*).

NMR experiments

The interaction between **L1** and the guest anions ($G = F^-$, Cl^-, Br^-, I^- and AcO^-) was investigated in DMSO-d_6–0.5% water solution at 298 K. The addition of F^-, Cl^- or AcO^- to **L1** gave rise to a significant ^1H NMR shift of the side-arm resonances, mainly of the ureido protons H5 and H7, while the spectra remain substantially unchanged after the addition of Br^- and I^- (Figure 1). In addition, the spectrum obtained by adding a large excess of NBu_4OH as a base clearly indicates the deprotonation of the urea groups affording the complete disappearance of the ureido protons as well as the upfield shift of the phenyl protons H1 and H3. Notably, receptor **L2** in the presence of a small amount of F^- (0.5 equivalent with respect to **L2**) gave rise to the disappearance of both ureido proton signals due to the deprotonation process (*12*); this does not occur with **L1** in which both signals, although broad, are visible in the ^1H NMR spectrum even when more than 2 equivalents of the anion were added (Figure 1). In addition, the peak resulting from the formation of the $[FHF]^-$ species, usually confirming the deprotonation process (*12*), appears only in the presence of a very large excess of F^- as a broad

Table 1. Logarithms of the association constants of the guests ($G = F^-$, Cl^-, Br^- and AcO^-) to **L1**, determined by UV–vis, fluorescence and NMR titration in DMSO-d_6–0.5% water solution or CH_3CN at 298 K.

	Log *K*				
		CH_3CN			
Reaction	DMSO AcO^-	AcO^-	F^-	Cl^-	Br^-
$L + G = LG$	4.5(1)[a]	6.5(1)[b] 6.7(1)[c]	5.4(1)[b] 5.6(1)[c]	4.6(1)[b] 4.7(1)[c]	3.4(1)[b] 3.4(1)[c]
$LG + G = LG_2$	2.1(1)[a]	3.9(1)[b] 4.0(1)[c]	5.1(1)[b] 5.3(1)[c]	3.4(1)[b] 3.4(1)[c]	2.9(1)[b] 2.8(1)[c]

Note: Values in parentheses are the standard deviation to the last significant figure.

[a] Values obtained by NMR.

[b] Values obtained by UV–vis.

[c] Values obtained by fluorescence experiments.

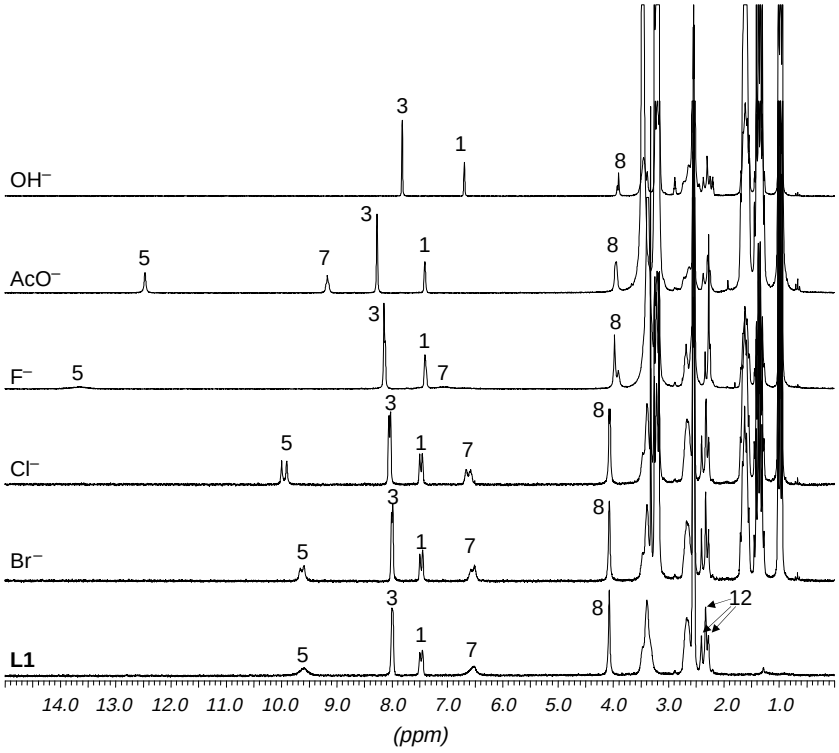

Figure 1. ^{1}H NMR spectra of **L1** in DMSO-d_6–0.5% water solution at 298 K by adding 3 equivalents of the guest with respect to **L1**, with the exception of OH^- added in large excess; the addition of I^- does not modify the **L1** spectrum.

triplet at 16.1 ppm. In other words, the urea fragment is less acidic in **L1** than in **L2**. Unfortunately, the broad lines of the ureido resonances in the **L1**/F^- system did not allow the obtainment of reliable association constants for this system.

Another aspect to be highlighted by NMR spectra of **L1** is the opposite shift exhibited by H3 with respect to H1 protons in the presence of the interacting anions (Figure 1). For example, at the end of the titration with AcO^-, H3 is 0.28 ppm downfield shifted while H1 is 0.06 ppm upfield shifted with respect to the free **L1**; on the contrary, by adding an excess of OH^-, i.e. deprotonating the urea units, both H1 and H3 exhibit upfield shifts of 0.82 and 0.19 ppm, respectively. The different behaviour of H3 in the presence of interacting or deprotonating anions is due to a different process occurring at the TFP–ureido group. In the adduct with anion, the shift is in agreement with the statement that the host–guest interaction occurs at the ureido group; this mainly affects the hydrogen atoms in the *ortho* position to the TFP group via a through-space interaction (*13*), a similar trend is exhibited by H3 in the presence of F^- and Cl^-, with downfield shifts of 0.14 and 0.06 ppm, respectively. The deprotonation of the ureido fragment mainly affects the hydrogen atoms H1 in the *para* position to the TFP group due to a mesomeric effect favoured by the deprotonation of the nitrogen atom closer to the TFP group.

The ^{1}H NMR experiments carried out in CD_3CN solution showed a similar behaviour, although the spectra resulted just a bit sharper and shifted; in addition, Br^- also affects the ^{1}H NMR spectrum in a similar way to the other anions (Figure 2).

It is interesting to observe that the ligand **L1** exhibits a complex number of signals in both solvents. In particular, in CD_3CN, it displays three resonances for the two methyl groups (H12) of the macrocyclic base (Figure 2), which, together with the number of all aliphatic resonances in the ^{13}C NMR spectrum (see Experimental Section and Figure S2 of the Supporting Information, available online), suggests the existence of two slowly interchanging conformers in solution, on the NMR time scale. The 1:1 mixture of conformers is produced by the rotational restriction of the amide groups of the tetraaza base (*14*). Looking at the aromatic H1 and H3 as well as at the ureido H5 and H7 and methylene H8 protons, they all exhibit twice the number of signals expected by their equality on the NMR time scale.

Assuming that only two distinct resonances are observed for each side arm vs. a total of a possible four, two possible explanations for this pattern of signals can be hypothesised. In the first one, the two side arms are equivalent inside the same conformer but not equivalent among the two conformers (a); the second one is contrary, i.e. the two side arms are equivalent among the two conformers but not equivalent inside the same

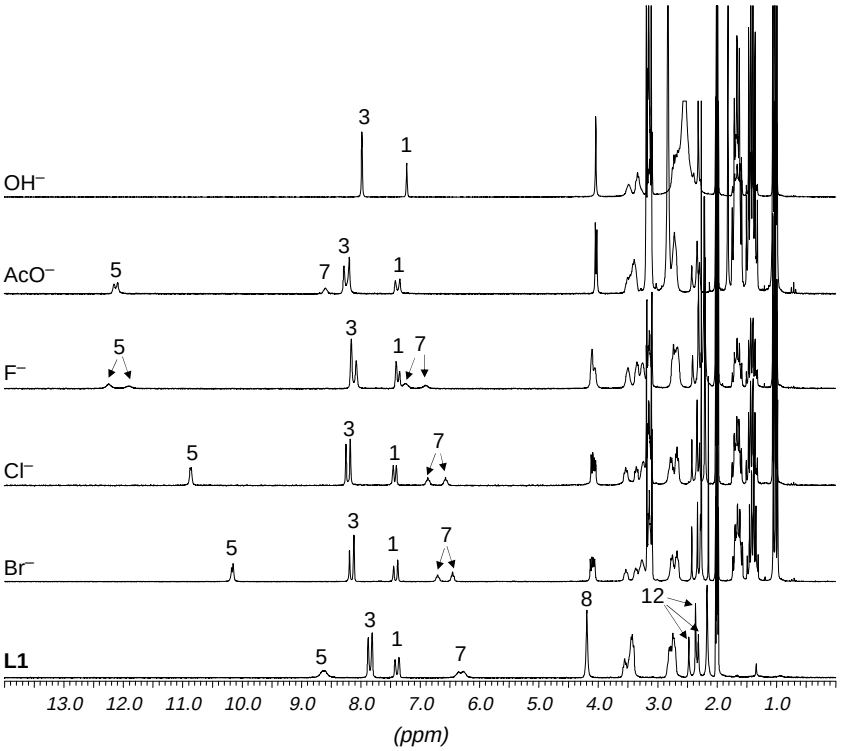

Figure 2. ^{1}H NMR spectra of **L1** in CD_3CN solution at 298 K by adding 3 equivalents of the guest with respect to **L1**, with the exception of OH^- added in large excess; the addition of I^- does not modify the **L1** spectrum.

conformer (b); both hypotheses are schematically reported in Figure 3.

^{1}H NMR experiments at variable temperatures in both solvents were carried out. In DMSO-d_6, the resonances of the side arms collapse in only one pattern of signals at $T = 333$ K (Figure 4); at this temperature, the resonances of the macrocyclic base are still broad. The resonances of the side arms preserve the same linewidth at higher temperature while the macrocyclic resonances collapse in a sharp pattern of signals, resulting from a C_{2v} symmetry mediated on the NMR time scale, at 353 K (Figure 4). In other words, the side arms become equivalent at lower temperature than the macrocyclic base, on the NMR time scale, independent of two conformers, thus the second hypothesis (b) seems to be the most likely one (see Figure 3(b)). In addition, the NMR titrations performed considering all the shifting signals separately yield comparable stability constants, supporting the previous statement. The spectra at variable temperatures carried out in CD_3CN showed a similar trend but, due to the lower boiling point of the solvent, the complete collapse of all resonances was not achieved.

^{19}F NMR can be carried out to follow the behaviour of CF_3 groups in the presence of anions in both solvents; for example, in DMSO-d_6, they show two singlets at -62.0 and -61.84 ppm due to the non-equivalence of the two side arms on the NMR time scale. The formation of the adducts with acetate as well as with fluoride gives rise to a small downfield shift of the resonances which collapse in only one singlet at -61.69 and -61.53 ppm for AcO^- and

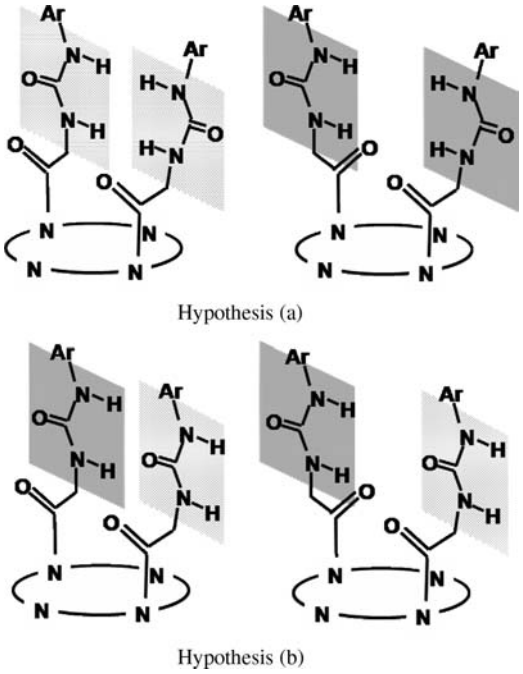

Figure 3. Schematic drawing of the possible conformers.

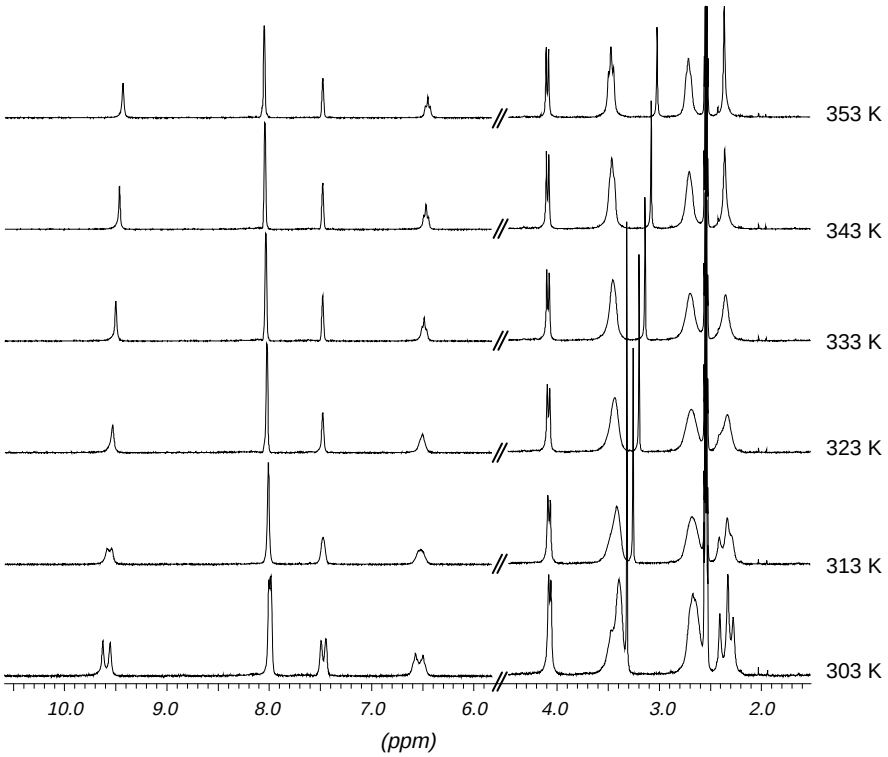

Figure 4. ^{1}H NMR spectra of **L1** species, recorded in DMSO-d_6 solution at different temperatures.

F^-, respectively (see Figure S1 of the Supporting Information). In the case of fluoride, it is possible to highlight the interaction with **L1** following the signal exhibited by F^- in the ^{19}F NMR spectra; the free F^- shows a sharp resonance at -97.4 ppm. By adding increasing equivalents of **L1** to the F^- solution, the signal becomes broader and shifts downfield up to -87.6 ppm in an excess of the host (all F^- bound; see Figure S1 of the Supporting Information); however, only one resonance is observable even at different **L1**/F^- molar ratios, indicating a fast exchange between coordinated and free fluoride on the NMR time scale. A similar behaviour was observed in CD_3CN where the signal of fluoride shifts from -111.5 to -88.7 ppm in the presence of a large excess of **L1**.

In ^{1}H NMR, the interaction between F^- and **L1** in CD_3CN broadens the ureido resonances, preventing the accurate evaluation of the stability constants for the **L1**/F^- system (see Figure S3 of the Supporting Information). However, although very broad, the H5 and H7 signals still appear in the spectrum even when an excess of F^- was added (Figure 2 and see Figure S3 of the Supporting Information), suggesting that F^-, unlike DMSO, is not able to deprotonate the TFP–urea group in this medium. This is also supported by the lack of resonance resulting from the $[FHF]^-$ species.

As shown in Figures 1 and 2, the shift of both ureido protons in the presence of halides is in agreement with the H-bonding acceptor power of the anion, the highest for F^- and the lowest for Br^-. A marked downfield shift in the H7 resonance, compared to the halides, was observed in the presence of AcO^- anion in both media. This accentuated shift of H7 with AcO^- can be attributed to the different way that **L1** stabilises the two different anions, i.e. spherical vs. V-shape.

In conclusion, the NMR experiments proved that the replacement of PNP with TFP in **L1** preserves the behaviour of this class of receptors in binding anions. The TFP groups decrease the acidity of the ureido fragments but increase the solubility of the receptor in other solvents different from DMSO. A remarkable result is the ability of **L1** to form stable adducts with F^- in CD_3CN, unobtainable in DMSO.

UV–vis experiments

The UV–vis absorption spectrum of **L1** can be affected by the host–guest interaction with anions in CH_3CN, while it is not in DMSO. In DMSO solution, only the deprotonation of the TFP–urea groups, obtained by adding a large amount of hydroxide or fluoride anions, is able to change the spectral feature of **L1**. In these cases, the absorption profile shows two main bands at λ_{max} 261 nm ($\varepsilon = 20{,}900\,cm^{-1}\,mol^{-1}\,dm^3$) and 296 nm ($\varepsilon = 4800\,cm^{-1}\,mol^{-1}\,dm^3$) in the neutral ligand and a band at λ_{max} 305 nm ($\varepsilon = 30{,}500\,cm^{-1}\,mol^{-1}\,dm^3$) by adding OH^- or F^- in large amount with respect to **L1** due to the

deprotonated species. On the contrary, also in CH_3CN, the presence of interacting anions affects the UV–vis spectral profile of free **L1**; in particular, this occurs with the addition of acetate, fluoride, chloride and bromide, but not iodide. Performing titration experiments, it was possible to spectrophotometrically determine the association constants of G (AcO^-, F^-, Cl^- and Br^-) to **L1** (Table 1). An example of the UV–vis experiments is shown in Figure 5(a). The free **L1** in CH_3CN shows a spectrum with two main bands, with λ_{max} at 246 nm ($\varepsilon = 32{,}700\,cm^{-1}\,mol^{-1}\,dm^3$) and 291 nm ($\varepsilon = 3000\,cm^{-1}\,mol^{-1}\,dm^3$); when increasing amounts of AcO^- were added to **L1**, the two λ_{max} shifted towards lower energies reaching, after the addition of about 4 equivalents of AcO^- (see the inset of Figure 5(a)), the maximum shift at λ_{max} 252 nm ($\varepsilon = 33{,}600\,cm^{-1}\,mol^{-1}\,dm^3$) and 295 nm ($\varepsilon = 3400\,cm^{-1}\,mol^{-1}\,dm^3$). This spectral change is attributed to the formation of **L1**–AcO^- adducts able to affect the

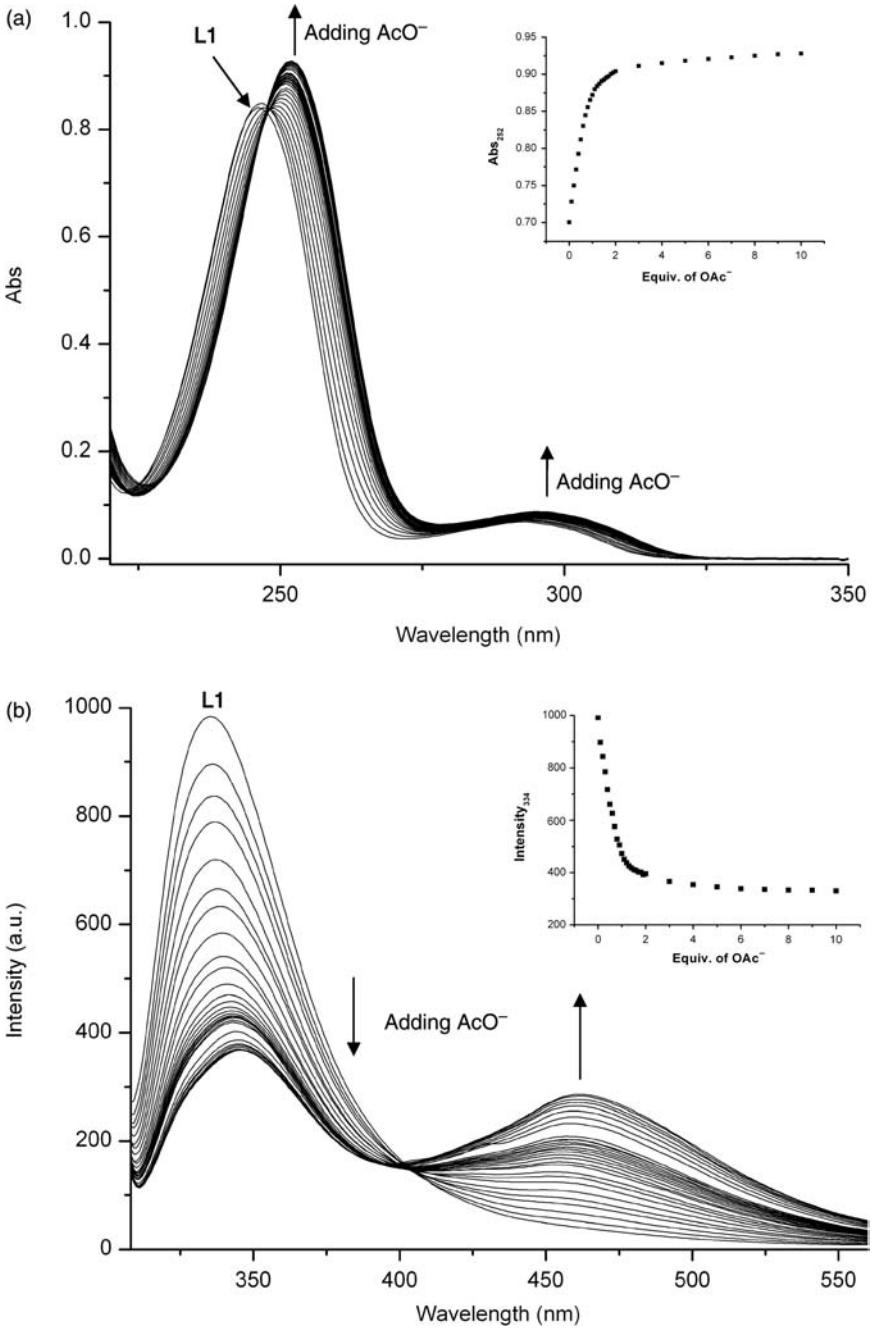

Figure 5. (a) UV–vis [**L1**] = 2.5×10^{-5} M and (b) fluorescence titration [**L1**] = 2.5×10^{-6} M of **L1** with AcO^- in CH_3CN solution at 298 K. Inset: variation of the λ_{abs} at 252 nm and λ_{em} at 334 nm as a function of AcO^- added.

chromophore in this medium. No deprotonation process was observed in the presence of a large amount of the guest by UV–vis experiments confirming the NMR experiments. In this solvent, the deprotonation of the ureido units can be obtained only by adding a strong base such as NBu_4OH, which yields a decrease in the band near 250 nm with the simultaneously strong increase in that near 300 nm with an eight-fold increase in absorptivity (see below).

This different optical response of the TFP–ureido chromophore to the presence of anions in the two solvents can be ascribed to the formation of stronger H-bond interactions in CH_3CN than in DMSO due to the different dielectric constant of the solvents (*11*) and in agreement with the ^1H NMR results.

The addition of F^-, Cl^- and Br^- to the CH_3CN solution containing **L1** gives rise to UV–vis absorption results similar to those obtained with AcO^- (Figure 6(a)), with the shift of

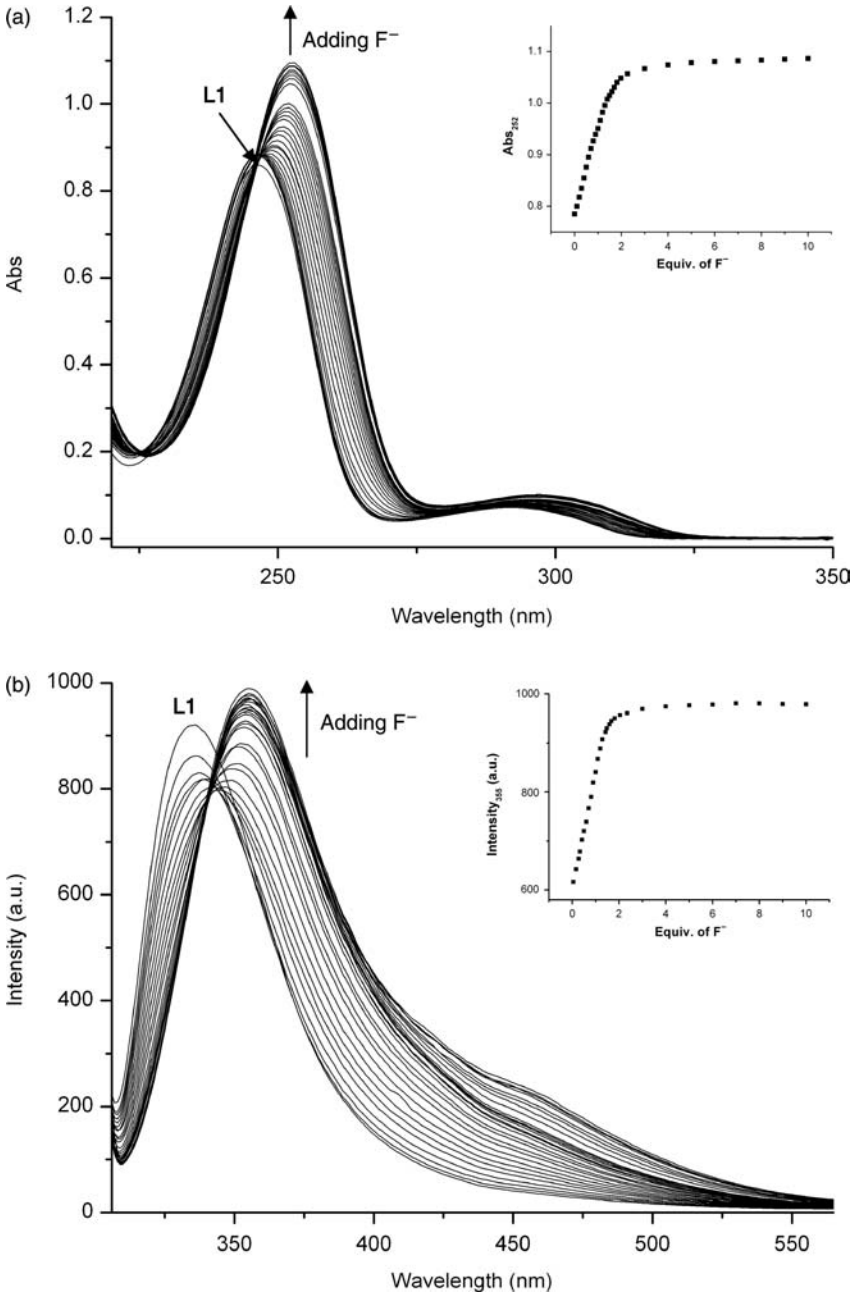

Figure 6. (a) UV–vis [**L1**] = 2.5×10^{-5} M and (b) fluorescence titration [**L1**] = 2.5×10^{-6} M of **L1** with F^- in CH_3CN solution at 298 K. Inset: variation of the λ_{abs} at 252 nm and λ_{em} at 355 nm as a function of F^- added.

both bands reaching their maximum shift at λ_{max} 253 nm ($\varepsilon = 36{,}200\,cm^{-1}\,mol^{-1}\,dm^3$) and 249 nm ($\varepsilon = 32{,}500\,cm^{-1}\,mol^{-1}\,dm^3$), 247 nm ($\varepsilon = 31{,}400\,cm^{-1}\,mol^{-1}\,dm^3$) and 297 nm ($\varepsilon = 3800\,cm^{-1}\,mol^{-1}\,dm^3$), 293 nm ($\varepsilon = 3200\,cm^{-1}\,mol^{-1}\,dm^3$) and 292 nm ($\varepsilon = 3100\,cm^{-1}\,mol^{-1}\,dm^3$) for F^-, Cl^- and Br^-, respectively. The invariance of the spectra was observed after the addition of about 3, 5 and 7 equivalents of F^-, Cl^- and Br^-, respectively. The shift of λ_{max}, as well as the equivalents of the anion necessary to saturate the spectra, highlights that the affinity of **L1** towards the halide series depends on their H-bonding acceptor affinity, the highest for fluoride and the lowest for bromide. In agreement with the NMR experiments, no deprotonation process was observed with the halide series, neither with F^-, in CH_3CN, even when adding a large excess of the anion with respect to **L1**; this highlights that, in CH_3CN, only the association between **L1** and the halide series takes place.

This is an important aspect which allows, processing the titration curves, the evaluation of the association constants of adducts formed with fluoride. The data for all **L1**–G adducts formed, obtained by UV–vis titration, are reported in Table 1 and are discussed below. It is interesting to underline a further difference of **L1** in the two solvents in the presence of OH^-. The addition of OH^- to a DMSO solution of **L1** does not significantly affect the two bands (shift < 1 nm) when adding up to 10 equivalents of OH^- with respect to **L1**; moreover, at least 100 equivalents of OH^- are able to deprotonate the urea group. On the contrary, the titration in CH_3CN shows the red shift of both bands, similar to that exhibited by adding acetate; they shift from 246 and 291 to 252 and 294 nm, respectively, in the presence of 10 equivalents of OH^- (Figure 7(a)). In other words, as reported for other anions, OH^- first interacts with **L1** via H-bond and then, only when it is present in large excess, it deprotonates the TFP–urea units. Probably, this occurs in both solvents but it is more evident in CH_3CN where, similar to results obtained with the other anions, the H-bonds formed in the **L1**–G adducts are stronger and are thus able to modify the spectral feature of **L1**. Unfortunately, either the association constant is too high or the deprotonation and association processes occur simultaneously and they are not independent since we were not able to safely determine their constant values by the spectrophotometric titrations.

Performing experiments at a fixed concentration of OH^-, we found that $[OH^-] \geq 10^{-3}$ M is able to deprotonate **L1** in DMSO while, with $[OH^-] \leq 10^{-4}$ M, **L1** remains in its neutral form. The range found in CH_3CN is 10-fold higher; in fact, only $[OH^-] \geq 10^{-2}$ M is able to deprotonate **L1** while it is in the neutral form for $[OH^-] \leq 10^{-3}$ M. This in addition to highlighting the lower acidity of **L1** in CH_3CN than in DMSO, as expected, provides a range of $[OH^-]$ in which **L1** can be used as a sensor for a strong base.

Fluorescence experiments

The presence of the TFP groups makes **L1** fluorescent in both DMSO and CH_3CN solvents. In DMSO, in agreement with UV–vis absorption properties, the fluorescence is only sensitive to the deprotonation process while it is not to the interaction with the anions. By excitation at 291 nm in DMSO, the free ligand shows an emission band centred at 350 nm (quantum yield $\Phi = 0.010$), while the deprotonation process gives rise to a new band with $\lambda_{em} = 481$ nm having a five-fold enhancement in the emission when compared to that at 350 nm. The higher energy band is attributed to the neutral form of **L1** while the lower energy band is attributed to the deprotonated one.

On the contrary, the fluorescence of **L1** in CH_3CN is modified by the presence of the interacting anions. The free **L1** exhibits an emission band with λ_{em} at 334 nm (quantum yield $\Phi = 0.013$, $\lambda_{ex} = 296$ nm). By adding up to 10 equivalents of OH^- with respect to **L1**, a red shift of the band up to 346 nm, together with the appearance of a new band at lower energy ($\lambda_{em} = 463$ nm), can be observed; however, the emission of this latter remains lower than that of the former. Adding a large excess of OH^-, the disappearance of the band at higher energy, together with a further shift of the band at lower energy ($\lambda_{em} = 480$ nm), can be observed, with a five-fold enhancement of the emission with respect to that at 334 nm (Figure 7(b)). The first trend of the titration is similar to that found for the halides (Figure 6(b)), confirming, as reported above for the absorption properties, that OH^- first interacts with **L1** via H-bond and then, only when it is present in large excess, it is able to deprotonate the TFP–urea units. It must be highlighted that, in CH_3CN, the emission bands of both neutral and deprotonated ligands are centred at higher energies with respect to those in DMSO. This means that, being the absorption transition, an $n \rightarrow \pi^*$ charge transfer, the higher dielectric constant of DMSO better stabilises the excited state with respect to CH_3CN, thus increasing the Stoke shift.

The different wavelength of emission exhibited by free and deprotonated ligands in both solvents is well visible not only by the spectral profile but also to the naked eyes, irradiating two different samples with UV light, one containing only **L1** and the other **L1** plus hydroxide anion (see Figure 8). The two bands can be attributed to the emission of the neutral and deprotonated forms of the TFP–urea group, respectively, making **L1** sensitive to the presence of OH^-, although in large excess when compared to **L1**. **L1** responds to the presence of OH^- by visible fluorescent emission in the same $[OH^-]$ range as in the UV–vis experiments, suggesting that it could be a possible application for **L1**; a fluorescent sensor for OH^- or another strong base able to deprotonate the TFP–ureido

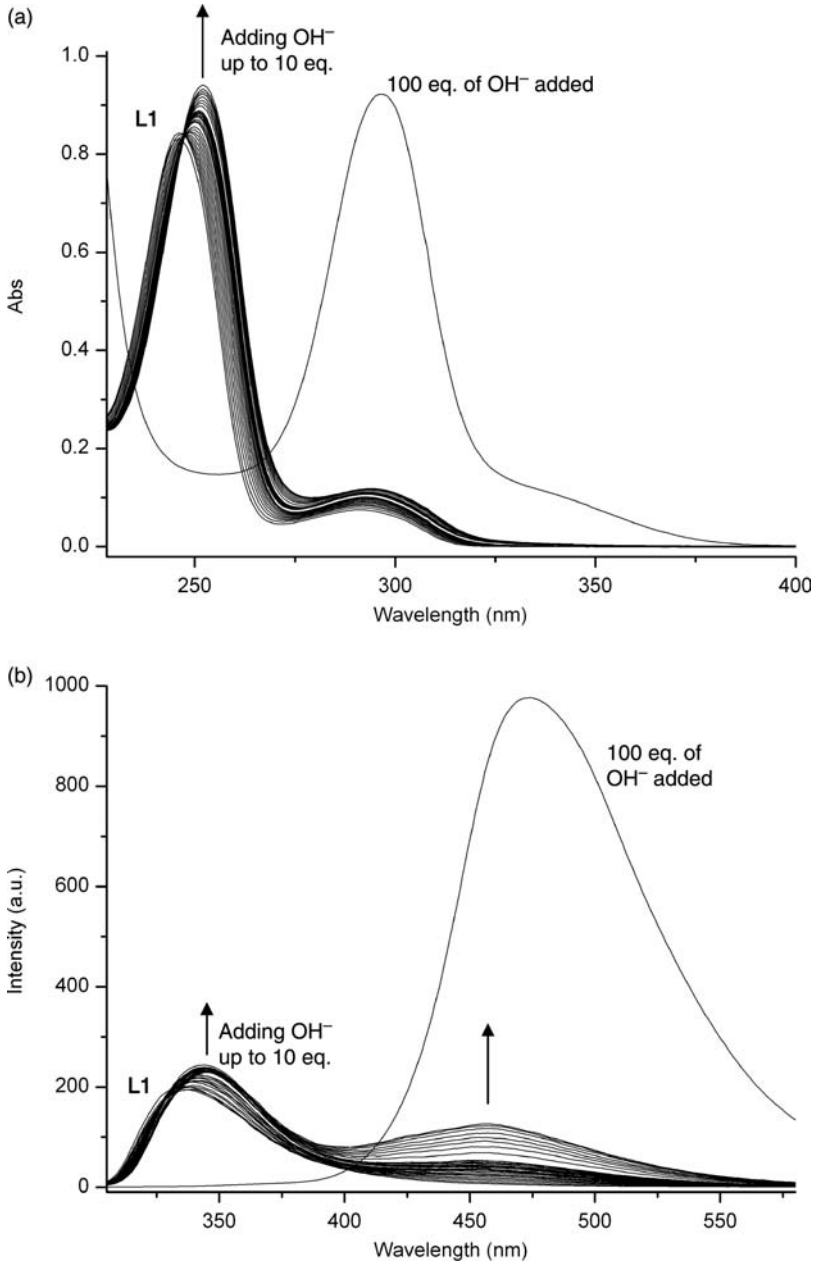

Figure 7. (a) UV–vis [**L1**] = 2.5×10^{-5} M and (b) fluorescence titration [**L1**] = 2.5×10^{-6} M of **L1** with OH^- in CH_3CN solution at 298 K.

unit in non-aqueous solvents. As mentioned above and in agreement with the UV–vis experiments, the fluorescence spectrum is affected by the presence of AcO^-, F^-, Cl^- and Br^- anions while I^- does not affect the fluorescence of **L1**, suggesting the lack of interaction between **L1** and iodide.

Figure 5(b) reports the titration of **L1** with acetate; as can be seen, the λ_{em} at 334 nm decreases when adding the anion while a new band centred at 457 nm appears in the spectrum. This band lies in the visible range, thus making **L1** suitable to detect the anion also with the naked eyes and the solution shows a colour similar to that reported in Figure 8. In the inset of Figure 5(b), it is possible to see that the band centred at 334 nm stops to vary after the addition of about 4 equivalents of AcO^-.

This spectral behaviour is attributed to the interaction via H-bonding of **L1** with AcO^- taking place at the ureido groups. Even when adding acetate, as a solid compound, no deprotonation process was observed in agreement with the NMR and UV–vis experiments. Examining the fluorescence of **L1** in the presence of F^- (Figure 6(b)), a different trend with respect to that observed with AcO^- can be highlighted. While the presence of acetate gives rise

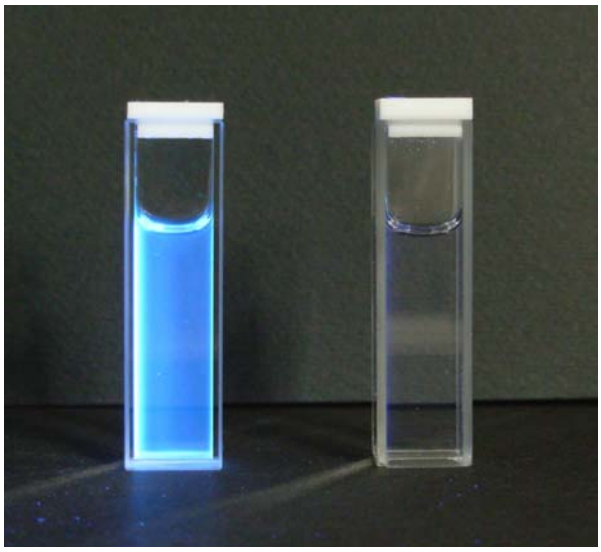

Figure 8. Photo of the sample of **L1** in CH_3CN solution: alone (right) and in $[OH^-] = 1 \times 10^{-2}$ M (left).

to the decrease in the emission at higher energy with the simultaneous appearance of a new band at lower energy, the presence of fluoride does not produce the appearance of the latter band ($\lambda_{em} = 457$ nm) but a marked red shift of the band at higher energy which moves from $\lambda_{em} = 334$ to $\lambda_{em} = 355$ nm (Figure 6(b)) with a slight increase in the emission; the spectrum obtained after the addition of 3 equivalents of fluoride is not further modified. A similar behaviour was also observed by adding Cl^- and Br^-, although with a lower shift of the band at $\lambda_{em} = 334$ nm (the final λ_{em} is 343 and 341 nm for Cl^- and Br^-, respectively). These data highlight that the emission of **L1** is affected in a different way by the presence of AcO^- vs. F^- and the other halides in solution; in particular, while the halides shift the λ_{em} of the neutral form of **L1**, and this shift can be correlated with the strength of H-bonding occurring, the highest shift for F^- and the lowest for Br^-, the acetate quenches the emission of this band and produces the appearance of a new band, with a wavelength similar to that of the deprotonated ones but of lower intensity. In other words, while the spectra of **L1** in the presence of halides show only one emission band, the presence of acetate gives rise to two distinct emission bands, one being of the neutral and another of the deprotonated species of **L1**. The hypotheses to explain this aspect, as already suggested in the NMR assays and also taking into account that no **L1** deprotonation was observed in NMR or UV–vis experiments in CH_3CN in the presence of AcO^-, could be a different way of coordination and thus a different H-bonding network provided by **L1** in stabilising the bidentate AcO^- vs. the spherical halides, in addition to the higher basicity of AcO^- that favours the deprotonation of the fluorophore in the excited state, as often reported in the literature in similar cases (*15*). However, it is to remark that the presence of AcO^- in solution can be signalled by fluorescence emission in the visible range ($\lambda_{em} = 457$ nm) which the other anions do not yield.

Association constants

All the G–**L1** titrations, carried out by UV–vis, fluorescence and when it was possible by ^{1}H NMR experiments, were processed and the stability constants of the species formed are summarised in Table 1. The constants evaluated by NMR titrations were obtained by processing all shifting resonances together or separately; no significant changes in the constant values were found. As reported above, in DMSO, only NMR is sensitive to the presence of the guests, while, in CH_3CN, the constants were obtained only from UV–vis and fluorescence data. The NMR experiments are not suitable, since the association constants with halides and acetate are too high in this medium (*16*). The processing of the ^{1}H NMR titration gave rise to the stability constants due to the formation of **L1**–AcO^- adducts in DMSO. The speciation of the adducts, as well as the values of the association constants, resulted similar to those obtained with the previously studied receptor **L2** (*6*); in fact, **L1** forms two adducts, $[\mathbf{L1}AcO]^-$ and $[\mathbf{L1}(AcO)_2]^{2-}$, with association constant values of $\log K = 4.5$ and 2.1, a bit lower but with a similar trend to those obtained with **L2** ($\log K = 5.6$ and 2.9 for the addition of the first and second acetate, respectively). The addition of the first acetate being higher than the second and higher with respect to a V-shape stabilisation by only one aromatic-ureido group in DMSO (*11*), a coordination of AcO^- in the $[\mathbf{L1}AcO]^-$ species similar to that suggested in the $[\mathbf{L2}AcO]^-$ species can be supposed (*6*). In other words, both side arms with both ureido groups participate in stabilising one AcO^- via H-bonding. As previously demonstrated (*14*), the key to preorganisation is given by the two N—C═O groups linking each side arm to the 12-membered macrocyclic ring, thus preorganising them so that both urea groups cooperate in stabilising the acetate via H-bond.

The speciation of adducts formed in CH_3CN is similar to that found in DMSO with acetate; in fact, **L1** forms adducts with the anion G of both $[\mathbf{L1}G]$ and $[\mathbf{L1}G_2]$ stoichiometries. The value of the association constants results higher for the addition of AcO^- in CH_3CN than in DMSO, as usually expected when using these solvents (*11*). In particular, the formation of both $[\mathbf{L1}AcO]^-$ and $[\mathbf{L1}(AcO)_2]^{2-}$ species resulted higher by about 2 logarithmic units in CH_3CN than in DMSO; moreover, the addition of the first acetate is higher than the second and higher with respect to a V-shape stabilisation of AcO^- by only one aromatic-ureido fragment. This again suggests

the cooperation of both side arms in stabilising the acetate in this solvent as well. The second acetate is stabilised by lower association constant; this can be attributed to the fact that both urea units are involved in the stabilisation of the first AcO^-, hindering the binding of the second acetate, once again indicating the cooperation of both side arms in binding the first AcO^-.

The stability constants with the halides, evaluated only in CH_3CN for shortness, show that **L1** is able to bind 2 equivalents of all the anions (Table 1), with similar association constants for the formation of the $[\mathbf{L1}G]^-$ and $[\mathbf{L1}G_2]^{2-}$ adducts. The similar values for the addition of the first and second anion suggest that the side arms probably behave independently in binding spherical guests such as the halide series. However, a small decrease in the association constant of the second anion can be observed with respect to the first one; these data can be ascribed to several contributions, even if difficult to determine. For example, the statistic effect, the second addition which takes place on a negatively charged species as well as the conformational changes of the ligand due to electrostatic repulsions in the negative $[\mathbf{L1}G_2]^{2-}$ adduct, could explain the lower value of the second constant. Nevertheless, the larger difference between the two stability constants observed in the case of chloride cannot completely exclude the participation of both side arms in the binding of the first chloride.

The values were higher for F^- than for Cl^- and higher for Cl^- than for Br^- in both steps, supporting the statement that the interaction occurs via H-bonding; in particular, fluoride exhibits very high association constants almost comparable to the addition of two acetates, although the latter shows the highest first association constant.

Conclusions

In this study, we have reported the synthesis and the binding properties of **L1**, a new versatile host for anions, both in DMSO and CH_3CN. Different synthetic approaches were investigated and the acyl-fluoride strategy was found to be the most reliable. An interesting one-pot procedure for the removal of the Cbz-protecting groups and formation of urea has also been performed. The present synthetic approach allowed to obtain the new receptor **L1** with a 54% overall yield, on a 10–15 mmol scale. Furthermore, the *N*-3,5-bis(trifluoromethyl)phenyl moiety was found to be fluorescent, extending the possibility to the determination of the host–guest interactions.

The anion coordination properties of the new receptor were investigated in solution by NMR, UV–vis and fluorescence spectroscopy; **L1** can bind AcO^-, F^- and Cl^- anions in DMSO solution and, in addition, Br^- in CH_3CN. The host–guest interaction occurs via H-bond at the TFP–ureido moieties; in DMSO, the receptor is sensitive to the presence of the anion only when employing ^1H and ^{19}F NMR, while, in CH_3CN, all the techniques explored are sensitive. The fluorescence in CH_3CN shows different spectral behaviours in the presence of AcO^- or halide anions; this can be attributed to a different way of stabilising the two guests by the side arms, in agreement with the stability constant values observed for the formation of the host–guest adducts. **L1** forms species of 1:1 ($[\mathbf{L1}G]$) and 1:2 ($[\mathbf{L1}G_2]$) stoichiometry with all the interacting anions. The higher value of the constant for the formation of the $[\mathbf{L1}AcO]^-$ species as compared to the $[\mathbf{L1}(AcO)_2]^{2-}$ one suggests that both side arms cooperate in binding this guest at least in the first complex but this does not occur with the spherical halide anion since the two association constants are similar. In other words, the cooperative effects of the two side arms can only be obtained with guests able to interact via H-bond in a bridge disposition with the two side arms, as in the case of the carboxylate group, whereas spherical anions, such as the halides, are more readily stabilised by only one side arm.

The stability constants resulted higher in CH_3CN than in DMSO, with AcO^- being the most strongly bound among all the anions investigated.

In conclusion, the introduction of the TFP group in this ligand topology enhances the handling and solubility in common organic solvents preserving the binding properties already found for this class of receptors. Moreover, the ability of **L1** to signal the presence of the acetate by significant fluorescence changes also in the visible range will stimulate us to develop the use of **L1** as a sensor for more complicated carboxylate guests.

Experimental section

General methods

IR spectra were recorded on a Shimadzu FTIR-8300 spectrometer. Melting points were determined on a Buchi melting point B 540 apparatus and are uncorrected. EI-MS spectra (70 eV) were recorded with a Fisons Trio 1000 spectrometer. The HPLC system (Waters Alliance 2795) was coupled with a photodiode array detector (Waters 2996 PDA), followed by an electrospray mass spectrometer detector (ESI-MS) (Waters-Micromass ZQ) worked by Mass Lynx 4.1 SP4 software. The ESI-MS analyses were performed in a positive mode under the following conditions: source and desolvation temperature, 100 and 250°C; capillary and cone voltage, 2.5 kV and 25 V; cone and desolvation flow (nitrogen gas), 40 and 400 l/h. HPLC analyses were performed on a 25 cm × 4.6 mm Discovery C-18, 5 cm column (Supelco, Bellefonte, PA, USA) equipped with a Supelguard Discovery C-18 guard column (2 cm × 4 mm, 5 cm).

Solvents A (MeOH) and C (5 nM ammonium acetate) were run at a flow rate of 1 ml/min. The running gradient was adjusted to 10% A (2 min), increasing to 90% A (18 min), and then 100% C (2 min), followed by a re-equilibration at 10% A (15 min). All solvents were HPLC grade (Aldrich-Sigma, Milwaukee, WI, USA) and water was purified via a Millex Q-plus system (Millipore, Bedford, MA, USA).

All chemicals were purchased from Aldrich, Fluka and Lancaster in the highest quality commercially available. All the solvents were dried prior to use. Chromatographic separations were performed on silica gel columns by flash chromatography (Kieselgel 60, 0.040–0.063 mm; Merck, Dr Whitehouse Station, NJ, USA). TLC analyses were performed on precoated silica gel on aluminium sheets (Kieselgel 60 F254, Merck). 1,7-Dimethyl-1,4,7,10-tetraazacyclododecane **3** was prepared as previously described (*17*).

Synthesis

*4(N),10(N)-Bis-[N-(benzyloxycarbonyl)glycyl]-1,7dimethyl-1,4,7,10-tetraazacyclododecane (**4**)*

To a well-stirred solution of *N*-Cbz-glycine **1** (56 mmol, 11.7 g) in dry CH_2Cl_2 (150 ml) and pyridine (56 mmol, 4.44 ml) kept under a N_2 atmosphere was added cyanuric fluoride (0.12 mol, 9.7 ml) at -20 to -10°C. A precipitate or emulsion was formed and gradually increased in amount. After stirring at -10°C for 2 h, crushed ice was added along with 300 ml of CH_2Cl_2. The organic layer was separated and the aqueous layer was extracted twice with 300 ml of CH_2Cl_2. The combined organic extracts were washed with 150 ml of ice-cold water, brine and dried (Na_2SO_4). The organic solution was filtered and concentrated under reduced pressure at room temperature to give the pure acid fluoride **2** (infrared carbonyl absorption 1847 cm^{-1}).

A solution of the above acid fluoride in dry CH_2Cl_2 (80 ml) was added dropwise over a period of 120 s at room temperature to a stirred solution of 1,7-dimethyl-1,4,7,10-tetraazacyclododecane **3** (4 g, 20 mmol) in 120 ml of H_2O containing 6.8 g (80 mmol) of $NaHCO_3$.

The mixture was stirred at room temperature for 60 min (after 50 min, IR examination showed the acid fluoride band at 1847 cm^{-1} to have essentially disappeared), followed by the addition of 350 ml of CH_2Cl_2. The organic yellow solution was separated and the aqueous layer was extracted twice with 200 ml of CH_2Cl_2.

The combined organic extracts were washed with 200 ml of brine, dried (Na_2SO_4) and concentrated under reduced pressure at room temperature to give compound **4** (10.3 g, 89% yield), which was used in the following step without further purification.

An analytical sample

Rotamer mixture: ^{1}H NMR ($CDCl_3$) $\delta = 2.24–2.38$ (6H, m), 2.63–2.71 (8H, m), 3.28–3.46 (8H, m), 4.05–4.07 (4H, m), 5.10–5.11 (4H, m), 5.82–5.89 (2H, m), 7.30–7.40 (10H, m); ^{13}C NMR ($CDCl_3$) $\delta = 42.8$, 43.1, 46.6, 55.0, 65.9, 127.2, 129.0, 141.2, 156.3, 164.3 ppm; FTIR (KBr): 3268, 3066, 2986, 2940, 1726, 1642, 1550, 1454, 1255, 1167 cm^{-1}; MS (+ESI) 583.7 (M + 1); Anal. for $C_{30}H_{42}N_6O_6$ (582.70): Calcd: C 61.84, H 7.27, N 14.42; Found: C 62.0, H 7.2, N 14.3.

*1,1′-(2,2′-(4,10-Dimethyl-1,4,7,10-tetraazacyclododecane-1,7-diyl)bis(2-oxoethane-2,1-diyl))bis(3-(3,5-bis(trifluoromethyl)phenyl)urea) (**L1**)*

Pd/C (10%, 2.1 g) was added to a solution of the above bis-carbamate **4** (10.3 g, 17.7 mmol) in EtOH abs (150 ml). The mixture was then hydrogenated at 1 atm with hydrogen balloon for 4 h at room temperature. When TLC showed disappearance of the starting material, 3,5-bis(trifluoromethyl)phenyl isocyanate **5** (40 mmol, 6.9 ml) was added at room temperature. After 2 h, the suspension was filtered through a short pad of Celite and the solvent was removed under vacuum. The solid thus obtained was purified on alumina using (CH_2Cl_2–MeOH 92:8) and then by silica gel column chromatography (CH_2Cl_2–MeOH–$NH_{3\,conc.}$ 91:8:1) to give the product **L1** as a white-off solid in 61% yield (9.7 g).

Rotamer mixture: mp = 226–228°C; FTIR (film): 3390, 2924, 1680, 1648, 1559, 1325, 1269, 1174, 1110 cm^{-1}; ^{1}H NMR (DMSO) $\delta = 2.31–2.47$ (6H, m), 2.71–2.85 (8H, m), 3.48–3.52 (8H, m), 4.12–4.17 (4H, m), 6.36–6.50 (2H, m), 7.34–7.38 (2H, m), 7.92–7.98 (4H, m), 9.11–9.18 (2H, m); ^{13}C NMR (DMSO): 41.5, 41.8, 46.6, 57.4, 118.6, 124.1(q), 129.1, 131.7, 140.3, 154.7, 167.8 ppm; MS (+ESI) 825.3 (MH+); Anal. for $C_{32}H_{36}F_{12}N_8O_4$ (824.67): Calcd: C 46.61, H 4.40, F 27.65, N 13.59, O 7.76; Found: C 46.65, H 4.45, N 13.69.

Spectroscopic experiments

^{1}H, ^{13}C and ^{19}F NMR spectra were recorded on a Bruker Avance 200 instrument, operating at 200.13, 50.33 and 188.31 MHz, respectively, and equipped with a variable temperature controller. The temperature of the NMR probe was calibrated using 1,2-ethanediol as a calibration sample. For the spectra recorded in $CDCl_3$, CD_3CN and DMSO-d_6, the ^{1}H and ^{13}C peak positions are reported with respect to TMS while $CFCl_3$ was used as a standard reference for the ^{19}F NMR spectroscopy. ^{1}H–^{1}H and ^{1}H–^{13}C correlation experiments were performed to assign the signals.

NMR titrations were carried out in CD_3CN or in a DMSO-d_6–0.5% water mixture; 0.5% of water was added

to DMSO to avoid the non-uniform absorption of water from the atmosphere by anhydrous DMSO during the titration. In a typical experiment, a 5×10^{-2} mol dm^{-3} solution of the anion was added in 0.1 eq at a time to a 1×10^{-2} mol dm^{-3} solution of the ligand directly in the NMR tube; the tube was then kept for 5 min at a temperature of 298 K before starting the acquisition of the spectrum. The anions tested were added as their tetrabutylammonium salts. The monitoring of the shift of the signals in the ligand spectra (see Results and discussion) permitted evaluation of the association constants of ligand–anion using the HYPNMR computer program (*18*).

Fluorescence spectra were recorded at 298 K with a Varian Cary Eclipse spectrofluorimeter. UV–vis absorption spectra were recorded at 298 K with a Varian Cary-100 spectrophotometer equipped with a temperature control unit. The interaction of anions with ligands **L1** and **L2** was studied in similar conditions of the NMR titration experiments using CH_3CN or DMSO-d_6–0.5% water mixture as the solvent; the solution containing the guest anion (F^-, Cl^-, Br^-, I^- or AcO^-) up to 5 equivalents with respect to the ligand was added to the solution containing **L1** ([**L1**] $= 1.5 \times 10^5$ M). At least three sets of spectrophotometric titration curves for each G/L system were performed. All sets of curves were treated either as single sets or as separate entities, for each system; no significant variations were found in the values of the determined constants. The HYPERQUAD computer program was used to process the spectrophotometric data (*18b*).

The fluorescence quantum yields (Φ_f) were determined by comparing the integrated fluorescence spectra of the sample with 2,2′-biphenol in acetonitrile ($\Phi_f = 0.29$) (*17*).

Supporting Information

^{19}F NMR titrations of **L1** with AcO^- or F^- in DMSO-d_6, ^{1}H NMR titration of **L1** with F^- in CD_3CN and ^{13}C NMR spectrum of **L1** are available online.

Acknowledgement

The authors thank the Italian Ministero dell'Istruzione dell'Università e della Ricerca (MIUR) PRIN2007 for the financial support.

References

(1) (a) Bianchi, A.; Bowman-James, K.; Garcia-España, E. *Supramolecular Chemistry of Anions*; Wiley-VCH: New York, 1997. (b) Sessler, J.L.; Gale, P.A.; Cho, W.S. *Anion Receptor Chemistry*; Royal Society of Chemistry: Cambridge, 2006. For recent reviews, see: (c) Caltagirone, C.; Gale, P.A. *Chem. Soc. Rev.* **2009**, *38*, 520–563. (d) Gale, P.A. *Acc. Chem. Res.* **2006**, *39*, 465–475. (e) Suksai, C.; Tuntulani, T. *Chem. Soc. Rev.* **2003**, *32*, 192–202. (f) Beer, P.D.; Gale, P.A. *Angew. Chem. Int. Ed.* **2001**, *40*, 486–516. (g) Schmidtchen, F.P.; Berger, M. *Chem. Rev.* **1997**, *97*, 1609–1646.

(2) Amendola, V.; Fabbrizzi, L. *Chem. Commun.* **2009**, 513–531.

(3) (a) Miranda, C.; Escarti, F.; Lamarque, L.; Yunta, M.J.R.; Navarro, P.; Garcia-España, E.; Jimeno, M.L. *J. Am. Chem. Soc.* **2004**, *126*, 823–833. (b) Lamarque, L.; Navarro, P.; Miranda, C.; Aran, V.J.; Ochoa, C.; Escarti, F.; Garcia-España, E.; Latorre, J.; Luis, S.V.; Miravet, J.F. *J. Am. Chem. Soc.* **2001**, *123*, 10560–10570.

(4) (a) Kang, S.O.; Begum, R.A.; Bowman-James, K. *Angew. Chem. Int. Ed.* **2006**, *45*, 7882–7894. (b) Esteban-Gomez, D.; Fabbrizzi, L.; Licchelli, M.; Monzani, E. *Org. Biomol. Chem.* **2005**, *3*, 1495–1500. (c) Lowe, A.J.; Dyson, G.A.; Pfeffer, F.M. *Org. Biomol. Chem.* **2007**, *5*, 1343–1346. (d) Suhs, T.; König, B. *Chem. Eur. J.* **2006**, *12*, 8150–8157. (e) Andres, A.; Aragò, J.; Bencini, A.; Bianchi, A.; Domenech, A.; Fusi, V.; Garcia-España, E.; Paoletti, P.; Ramirez, J.A. *Inorg. Chem.* **1993**, *32*, 3418–3424.

(5) (a) Kang, S.O.; Hossain, M.A.; Bowman-James, K. *Coord. Chem. Rev.* **2006**, *250*, 3038–3052. (b) Bowman-James, K. *Acc. Chem. Res.* **2005**, *38*, 671–678. (c) Amendola, V.; Esteban-Gomez, D.; Fabbrizzi, L.; Licchelli, M. *Acc. Chem. Res.* **2006**, *39*, 343–353. (d) Gale, P.; Quesada, R. *Coord. Chem. Rev.* **2006**, *250*, 3219–3244. (e) Kim, T.H.; Choi, M.S.; Sohn, B.-H.; Park, S.-Y. *Chem. Commun.* **2008**, 2364–2366. (f) Lowe, A.J.; Dyson, G.A.; Pfeffer, F.M. *Eur. J. Org. Chem.* **2008**, 1559–1567. (g) Amendola, V.; Baiocchi, D.M.; Fabbrizzi, L.; Mosca, L. *Chem. Eur. J.* **2008**, *14*, 9683–9696.

(6) Formica, M.; Fusi, V.; Macedi, E.; Paoli, P.; Piersanti, G.; Rossi, P.; Zappia, G.; Orlando, P. *New J. Chem.* **2008**, *32*, 1204–1214.

(7) For selected reviews of (thio)urea-based organocatalysis, see: (a) Zhang, Z.; Schreiner, P.R. *Chem. Soc. Rev.* **2009**, *38*, 1187–1198. (b) Connon, S.J. *Chem. Commun.* **2008**, 2499–2510. (c) Doyle, A.G.; Jacobsen, E.N. *Chem. Rev.* **2007**, *107*, 5713–5743. (d) Taylor, M.S.; Jacobsen, E.N. *Angew. Chem., Int. Ed.* **2006**, *45*, 1520–1543. (e) Takemoto, Y. *Org. Biomol. Chem.* **2005**, *3*, 4299–4306. (f) Schreiner, P.R. *Chem. Soc. Rev.* **2003**, *32*, 289–296.

(8) Valeur, E.; Bradley, M. *Chem. Soc. Rev.* **2009**, *38*, 606–631.

(9) (a) Carpino, L.A.; Beyermann, M.; Wenschuh, H.; Bienert, M. *Acc. Chem. Res.* **1996**, *29*, 268–274 and reference therein. (b) Jedrzejczak, M.; Motie, R.E.; Satchell, D.P.N.; Satchell, R.S.; Wassef, W.N. *J. Chem. Soc., Perkin Trans. 2* **1994**, 1471–1479.

(10) White, J.M.; Rao Tunoori, A.; Turunen, B.J.; Georg, G.I. *J. Org. Chem.* **2004**, *69*, 2573–2576.

(11) Pérez-Casa, C.; Yatsimirsky, A.K. *J. Org. Chem.* **2008**, *73*, 2275–2284.

(12) Shenderovich, I.G.; Tolstoy, P.M.; Golubev, N.S.; Smirnov, S.N.; Denisov, G.S.; Limbach, H.H. *J. Am. Chem. Soc.* **2003**, *125*, 11710–11720.

(13) Boiocchi, M.; Del Boca, L.; Esteban-Gomez, D.; Fabbrizzi, L.; Licchelli, M.; Monzani, E. *Chem. Eur. J.* **2005**, *11*, 3097–3104.

(14) (a) Formica, M.; Fusi, V.; Giorgi, L.; Guerri, A.; Lucarini, S.; Micheloni, M.; Paoli, P.; Pontellini, R.; Rossi, P.; Tarzia, G.; Zappia, G. *New J. Chem.* **2003**, *27*, 1575–1583. (b) Ambrosi, G.; Dapporto, P.; Formica, M.; Fusi, V.; Giorgi, L.; Guerri, A.; Lucarini, S.; Micheloni, M.; Paoli, P.; Pontellini, R.; Rossi, P.; Zappia, G. *New J. Chem.* **2004**, *28*, 1359–1367. (c) Ambrosi, G.; Formica, M.; Fusi, V.; Giorgi,

L.; Guerri, A.; Lucarini, S.; Micheloni, M.; Paoli, P.; Rossi, P.; Zappia, G. *Inorg. Chem.* **2005**, *44*, 3249–3260.
(15) Sharma, A.; Shulman, S.G. *Introduction to Fluorescence Spectroscopy*; Wiley: New York, 1999.
(16) Jyotirmayee, M.; Pal, H.; Sapre, A.V. *Bull. Chem. Soc. Jpn* **1999**, *72*, 2193–2202.
(17) Ciampolini, M.; Dapporto, P.; Micheloni, M.; Nardi, N.; Paoletti, P.; Zanobini, F. *J. Chem. Soc., Dalton Trans.* **1984**, 1357–1362.
(18) (a) Frassinetti, C.; Gelli, S.; Sabatini, A.; Moruzzi, M.S.; Vacca, A. *Anal. Biochem.* **1995**, *231*, 374–382. (b) Gans, P.; Sabatini, A.; Vacca, A. *Talanta* **1996**, *43*, 1739–1753.